J. Wind Eng. Ind. Aerodyn. 153 (2016) 46–59

Contents lists available at ScienceDirect

Journal of Wind Engineering and Industrial Aerodynamics

journal homepage: www.elsevier.com/locate/jweia

Improvement and development of one- and two-dimensional discrete gust models using a large-eddy simulation model

C. Knigge *, S. Raasch

Institut für Meteorologie und Klimatologie, Leibniz Universität Hannover, Germany

ARTICLE INFO

Article history:
Received 31 July 2015
Received in revised form
15 February 2016
Accepted 7 March 2016
Available online 1 April 2016

Keywords:
Aircraft
Atmospheric boundary layer
Gust loads
Large-eddy simulation
Mean gust shape
Strong-wind event
Wind turbines

ABSTRACT

High resolution large-eddy simulations (LES) were carried out to simulate the turbulent flow of the atmospheric boundary layer during an idealized strong-wind event in order to verify discrete gust models like the one-minus-cosine law which are used in the design process of aircraft and wind turbines. Furthermore existing gust models will be improved and new analytical approaches will be developed to approximate gusts more accurately. Mean gust shapes of the three wind speed components are calculated by means of virtual measurements of the turbulent wind speed at different heights above ground to analyze both the one- and two-dimensional characteristics of discrete gusts. One-dimensional results of the mean gust shapes show significant differences compared to the classical one-cosine gust model like a steeper increase and decrease as well as a rather constant middle part. Results obtained from previous mast measurements, however, show the same main gust characteristics as the present LES gusts. Two-dimensional mean gust shapes have not been calculated from field measurements yet. The results obtained from the LES data show elliptically shaped contours with different aspect ratios for different gust diameters and heights above ground. For both, one- and two-dimensional mean gust shapes, mathematical approximations are presented as alternative approach to the classical gust models in order to be able to reproduce the mean gust shapes for future applications.

1. Introduction

The lowest part of the atmosphere, the atmospheric boundary layer (ABL), is characterized by its turbulence, which can be described as chaotic flow superimposed on the mean wind caused by the interaction of different sized eddies (e.g. Stull, 1988). Within the turbulence, strong wind pulses can occur. They are also known as wind gusts or, more simply, gusts. In connection with storms gusts have an enormous potential for damages on structures like bridges and wind turbines or may cause hazardous situations in air traffic. Storms which lead to strong gusts are typically thunderstorms or storms associated with a large-scale low-pressure systems. Especially strong low-pressure systems and the severe gusts associated with them cause intense economic and insured losses (e.g. Friderichs et al., 2009; Born et al., 2012).

Due to the complexity of the turbulence, different approaches exist to describe either the stochastic character of the turbulence with spectral models or the shape of occasional occurring wind peaks with discrete gust models. Gust models are applied in different scientific and technical fields. Two examples, which are of utmost importance for modern traffic and energy generation, are the design processes of aircraft and wind turbines. In both fields calculations of extreme loads caused by strong discrete gusts are based on rather simple models (see e.g. Frost et al., 1978; Hoblit, 1988; Burton et al., 2011) which have been used for many decades. Besides the development of wind energy turbines and aircraft, meteorological weather forecast systems which are using wind gust estimation (WGE) models (e.g. Friderichs et al., 2009; Born et al., 2012) and the rail traffic (e.g. Andersson et al., 2004) can be mentioned as further important fields of application of wind gust models.

In the present study, the focus lies on gusts affecting aircraft and gust models used in aircraft design processes. However, the results are also valid and applicable for the different application areas mentioned above. In the aircraft design process the so called 'one-cosine' (also: 'one-minus-cosine' or '1-minus-cosine') gust shape is part of the admission rules in the Federal Aviation Regulations for Transport (Part 25, FAR, 2012). This rather simple gust model describes the one-dimensional wind speed variation with time during a gust event and can be written as

$$u(t) = (A/2)(1 - \cos(2\pi t/T)), \quad (1)$$

where A is the amplitude and T is the duration period of the gust. This gust shape approximation was first introduced in the middle

* Corresponding author.
E-mail address: knigge@muk.uni-hannover.de (C. Knigge).

http://dx.doi.org/10.1016/j.jweia.2016.03.004

of the last century by Pratt and Walker (1954). They used flight measurements data to draw conclusions of the atmospheric influence on the aircraft. Assuming that Taylor's hypothesis of frozen turbulence is applicable, the time t in Eq. (1) can be replaced by the stream-wise coordinate in space x. In this way, it is possible to calculate the spatial extension of gusts from time-dependent data, e.g. obtained from mast measurements. Furthermore this relationship between time and space is useful for comparing time- with space-depending measurements. Since the 1950s, only few studies focused directly on the characteristics of discrete gusts in the atmosphere. Examples are analyzes of gust shapes calculated from mast measurements by Camp (1968), Kristensen et al. (1991), Verheij et al. (1992) and Bierbooms and Dragt (1999). The typical approach they used in their studies is to describe gust statistically by averaging a large number of detected gusts of a wind measurement. Camp (1968) and Verheij et al. (1992), for example, calculated mean gusts representing the typical gust characteristics, like their shape, of a specific height above ground and gust length. Although these measurements indicate more complex and partly different gust shapes than the one-cosine formulation, the standard regulations still contain the classical gust shape model as formulated in Eq. (1).

Besides the discrepancies between the applied one-cosine gust shape and the gust shapes obtained from mast measurements, a further disadvantage of the gust model is that it provides only one-dimensional information of the gust structure. For two-dimensional load calculations, the gust shape can either be assumed as uniform along the second dimension (at least along the investigated structure), or the gust can be cut off at a certain point. For the latter case, only a defined part of the structure (e.g. aircraft or wind turbine) is affected by the wind pulse and the gust has typically a sharp edge in crosswind direction. It is obvious that both methods do not agree with a realistic atmospheric gust. Atmospheric turbulence and, hence, gusts are highly three-dimensional. The consideration of all three or at least the two horizontal spatial directions in gust shape models would help to avoid the above approximations in the crosswind direction and, hence, to improve load calculations for structures.

Modern research methods like Dual-Doppler-Lidar measurements and large-eddy simulations (LES) provide multi-dimensional data of the turbulent flow. Both methods allow to resolve the atmospheric turbulence and, hence, gusts. Based on the multi-dimensional data sets provided by these methods, two different approaches and strategies concerning gust analysis can be followed: On the one hand they allow to verify and, if necessary, to improve existing one-dimensional gust models. On the other hand it is possible to examine multi-dimensional structures of gusts to develop multi-dimensional gust models.

In the present study, mean one- and two-dimensional gust shapes depending on the altitude and spatial extension of the gusts are examined. Since the horizontal extension of aircraft is large compared to its vertical extension, vertical structures of gusts are neglected and the focus in this study lies on gusts in the horizontal plane. All three components of the wind speed vector are considered in order to achieve a reliable estimate of the complete wind field. In addition, one-dimensional gust shapes are analyzed to compare and verify the simulated gust shapes with the mast measurement studies mentioned above. For both the one- and two-dimensional gust shapes obtained from LES data, analytical approximations are presented.

This paper is organized as follows. Section 2 gives an overview of the simulation model PALM, the numerical setup, and the meteorological conditions used in the simulation. The gust definition and the applied gust extraction method is explained in detail by selected examples in Section 3. Results are presented in Section 4. It is split into three parts: the description of one- and two-dimensional gust characteristics followed by a discussion. Conclusions, a summary and a short outlook are given in Section 5.

2. Numerical methods and meteorological conditions

The investigation of discrete gusts requires a turbulence resolving method like the LES used in the present study. The principal of the large-eddy simulation is based on scale separation. Large scales, which contain most of the turbulent kinetic energy, are directly computed whereas small scales are modeled. The latter are also referred to as subgrid scales (SGS). Following this approach, the LES allows to simulates highly resolved three-dimensional flow fields of the ABL containing typical flow characteristics of the real ABL. In order to capture gusts, which are relevant for aircraft design processes, small-scaled turbulence structures, or gusts, which can affect airfoils of aircraft, must explicitly be simulated. Assuming a wing span of a commercial aircraft of about 30 m (e.g. Airbus A320) and that the effective resolution is about four times the grid spacing, a model resolution of 2 m was chosen for this study.

After introducing the applied LES model PALM, the meteorological scenario with the numerical setup and the boundary conditions are explained in detail.

2.1. PALM – a parallelized LES Model

The LES model PALM, revision 1048,[1] used for the investigations has been developed at the Institute of Meteorology and Climatology at the Leibniz Universität Hannover (Raasch and Etling, 1998; Raasch and Schröter, 2001). It is written in Fortran 95 and is used for simulations of the atmospheric (and oceanic) boundary layer. PALM was applied in several former studies to investigate different flow regimes in the convective boundary layer (CBL) and the neutral boundary layer (e.g. Letzel et al., 2008; Raasch and Franke, 2011; Schröter et al., 2000).

In the present study, PALM was used to simulate the dry atmosphere where it solves the non-hydrostatic, incompressible Boussinesq equations and the first law of thermodynamics. The equations are discretized using finite differences and are filtered implicitly following the volume-balance approach Schumann (1975). Turbulence closure uses the 1 $\frac{1}{2}$th order Deardorff (1980) scheme, which requires a prognostic equation for subgrid-scale turbulent kinetic energy (TKE).

Variables are located on a staggered grid (Arakawa C grid), where scalar quantities are defined on the cell centers and the velocity components on the borders of the cells (Arakawa et al., 1977; Harlow and Welch, 1965). Advection scheme is the fifth-order of Wicker and Skamarock (2002) and time integration uses the third-order Runge–Kutta scheme. The Monin–Obukhov similarity theory (MOST) is applied between the surface and the first grid level. This also includes the calculation of the friction velocity u_* from the roughness length and the local wind profiles. The simulations were carried out using cyclic lateral boundaries. A detailed description of PALM is available online (http://palm.muk.uni-hannover.de).

2.2. Setup of the scenario

One typical meteorological scenario associated with extreme wind gusts is a strong low-pressure system (extratropical cyclone). In Europe, they often occur as winter storms and are one of the

[1] The code can be accessed under http://palm.muk.uni-hannover.de/browser/?rev=1048.

most costly natural disaster (Born et al., 2012; Friderichs et al., 2009). A well known example of a severe winter storm is the storm "Kyrill", which occurred in January 2007. The main source of the strong turbulence in the boundary layer during such a storm event is the wind shear caused by the high magnitude of the undisturbed free stream above the boundary layer (geostrophic wind) and the surface friction. In the simulations, the top of the boundary layer was fixed at about $z_i = 700$ m with a temperature inversion. The gradient of the potential temperature above z_i was $\partial\theta/\partial z = 2$ K/100 m. The boundary layer itself was neutrally stratified. This stratification allows to fix the height of the boundary layer at a certain height level and, hence, to stretch the vertical grid above (in the stable layer) to reduce computational costs. Grid stretching was used from $z = 800$ m up to the model domain top at $z = 1800$ m. The chosen value of the inversion height z_i is large enough to ensure a realistic development of the boundary layer, which contains all typical flow structures of a neutral boundary layer. Some characteristic vertical profiles will be shown at the end of the current section.

The grid resolution below $z = 800$ m was 2 m in all directions. It was chosen fine enough to be able to resolve gusts affecting wings of aircraft or wind turbine blades. The model domain length is 2048 m in both horizontal directions. With the grid resolution mentioned above the number of grid points is $1024 \times 1024 \times 448$ ($x \times y \times z$).

For the stream-wise geostrophic wind component u_g, a geostrophic wind speed of 30 m s^{-1} was used. The chosen roughness length z_0 of 0.5 m corresponds the value of z_0 of a suburban area and can be seen as representative for typical surroundings of airports which are located near cities. The latitude used in the simulation is 55°.

The complete simulated time period was four hours. Data were extracted after a transient phase of one hour, when a quasi-stationary state over time was reached. Instantaneous three-dimensional flow fields of all three velocity components were stored every five minutes. A total of 24 points in time provide a large amount of data and thus allows a sufficient statistics of the calculated mean gust shapes (at each point in time, several hundreds of gusts could be extracted, see next section). The mean flow conditions during one and three hours simulation time are illustrated by the vertical profiles in Fig. 1. All mean profiles are both space- and time-averaged. Therefore, horizontal averages over the entire model domain (indicated by angular brackets) were calculated every five minutes during the specified period and averaged in time (indicated by bars). The above mentioned initial profiles of the horizontal velocity components and the potential temperature are shown in Fig. 1(a), (b) and (d). Indicated by the dotted line is

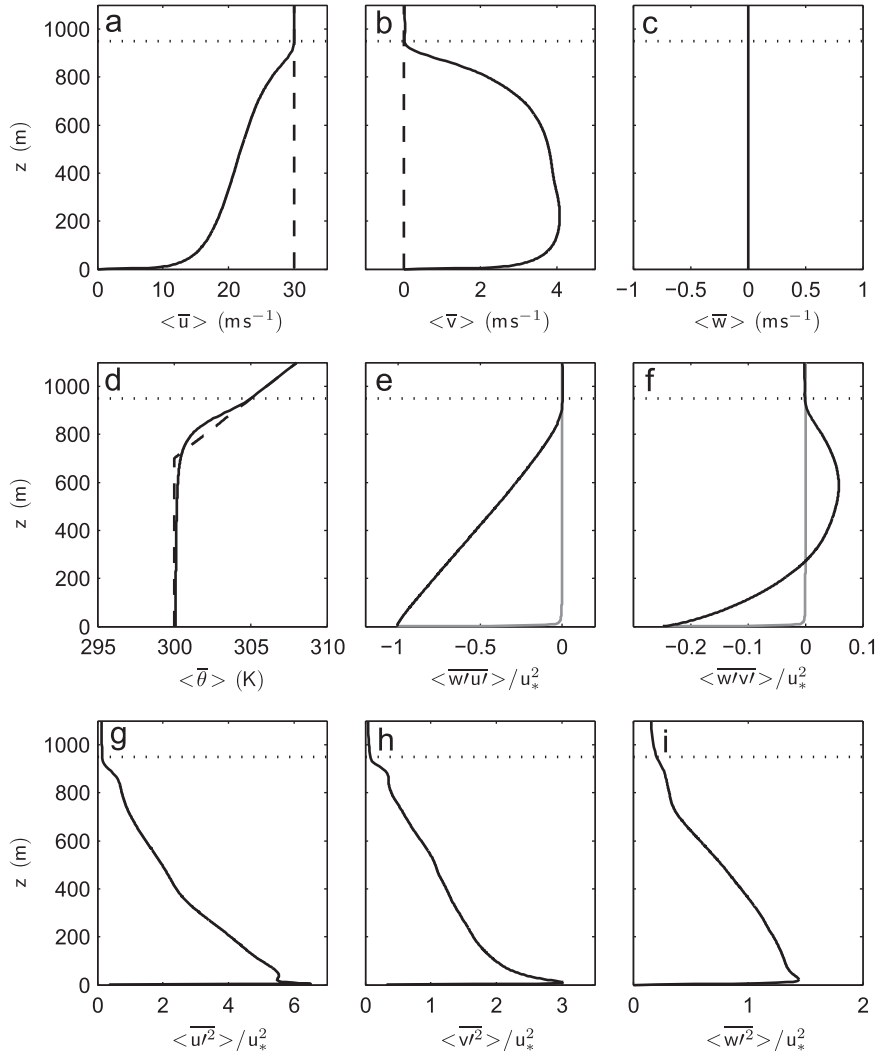

Fig. 1. Profiles describing mean flow and turbulence characteristics of the simulated atmospheric boundary layer: Mean (solid black lines) and initial (dashed lines) profiles of the wind velocities (a)–(c) and the potential temperature (d); normalized stress (e), (f) and velocity variances (g)–(i). The gray lines in (e) and (f) indicate the calculated SGS-part of the stress.

the mean height of the bottom of the undisturbed free atmosphere, where the geostrophic wind speed values are reached ($z \approx 950$ m). The boundary layer grows with time due to entrainment of stable air at the inversion. Thus, it is slightly stabilized from above and the mean stratification of the boundary layer can be described as 'near-neutral' (see Fig. 1(d)).

To quantify the influence of the SGS model, its contribution on the solution is compared to the total magnitude of a quantity. Fig. 1(e) and (f) shows the vertical fluxes of horizontal momentum $<\overline{w'u'}>$ and $<\overline{w'v'}>$ normalized with the friction velocity u_*. The primed velocities denote fluctuations superimposed to the mean flow. Besides the total momentum fluxes (solid black lines), the subgrid-scale fluxes are shown (solid gray lines). Their contribution is significant only within a few meters above the surface. Below a height of 6 m, the subgrid fluxes contribute more than 10% of the total fluxes. At a 10 m height the SGS contributions are reduced to 4% of the total magnitude of the corresponding total fluxes. To ensure that the influence of the SGS model is minimized, the 10 m-level was used as lowest height level in the gust analyzes. The vertical profiles in Fig. 1(e) and (f) agree well with classical profiles of fluxes in a neutral boundary layer. Similarly, the normalized profiles of the velocity variances (Fig. 1(g)–(i)) show the typical curve shapes for a neutrally stratified ABL (see Mason and Thomson (1987) and Stull (1988)).

3. Analysis methods

For the gust analysis of this study, instantaneous velocity data were used. Thus, the method to analyze the flow fields differ from the method based on mast measurements in that way, that no time-depending information of the velocity components are considered. Instead, gusts length scales can be calculated directly from the instantaneous data which provide 'snapshot pictures' of the atmosphere and thus allow a direct space dependent analysis of flow structures. Accordingly, the spatial information of gusts presented here are not based on the Taylor hypothesis.

Before describing the methods for extracting discrete gusts from the simulation output in detail, a short overview of the turbulent flow field will be presented. Fig. 2 shows instantaneous three-dimensional flow fields of the stream-wise horizontal velocity component u (Fig. 2(a)) and the vertical velocity component w (Fig. 2(b)) after 1.5 h of simulation time. Three horizontal cross-sections at 10 m, 100 m and 300 m show some of the height levels of the later analysis which contain the typical flow structures of the different altitudes. The colors of the cross-sections are slightly brighter to distinguish them better from the vertical planes. Additionally, the profile of the corresponding horizontal mean of each velocity component is illustrated (to the right of each figure). In order to show turbulent structures in more detail, the areas do not show the total model domain (a quarter of the horizontal domain and approximately two third of the boundary layer height is shown). The altitude of 500 m corresponds to the maximum height level of the gust analysis. On Fig. 2(a), the increasing horizontal wind speed can clearly be seen. The mean profile in the lowest 100 m has the typical logarithmic shape. At a height of 500 m, about 75% of the magnitude of the geostrophical wind is reached (see also Fig. 1(a)). In the lowest cross-section, at 10 m height, turbulent streaks (see Drobinski and Foster, 2003) are visible in the horizontal velocity (Fig. 2(a)). With increasing heights above ground, flow patterns become larger. In the flow field of the vertical velocity (Fig. 2(b)), the elongation of structures is also visible, however, not to the same degree as in the horizontal flow field. This impression is additionally amplified by the different color scales used in the figures. The mean vertical velocity in the shown area reaches values close to zero.

To extract discrete gusts from the turbulent flow fields, a distinct definition of a gust is required, however, no consistent definition of gusts exists in literature. It differs in the various disciplines like weather forecast and design of wind turbines or aircraft (see e.g. Friderichs et al., 2009; Hau, 2006; Hoblit, 1988). Most of the definitions in practical investigations have in common, that they use thresholds for the amplitude (typically a few meters per second as the deviation from zero or the mean wind) and the duration (typically a few seconds). The definition used in this study is based on these two parameters. Instead of the duration, the gust length or diameter, which could directly be determined, was used. Since the focus lies on gusts that have the potential of affecting aircraft of a significant amount, only gusts with a spatial extension between the typical wing span of commercial aircraft (approximately 30 m) and 150 m were considered. The minimum amplitude A_{min} is fixed at 3 m s^{-1} to ensure that only relatively strong wind pulses are extracted from the turbulent flow field.

From the instantaneous three-dimensional velocity data of the LES, horizontal cross-sections at seven different heights (10 m, 30 m, 50 m, 100 m, 200 m, 300 m, and 500 m) were used for both one- and two-dimensional gust analysis. The different methods applied to extract one- and two-dimensional gusts from the turbulent flow fields are described in the following subsections.

3.1. One-dimensional gust extraction method

In order to extract one-dimensional gust information from the two-dimensional instantaneous wind fields, virtual spatial wind

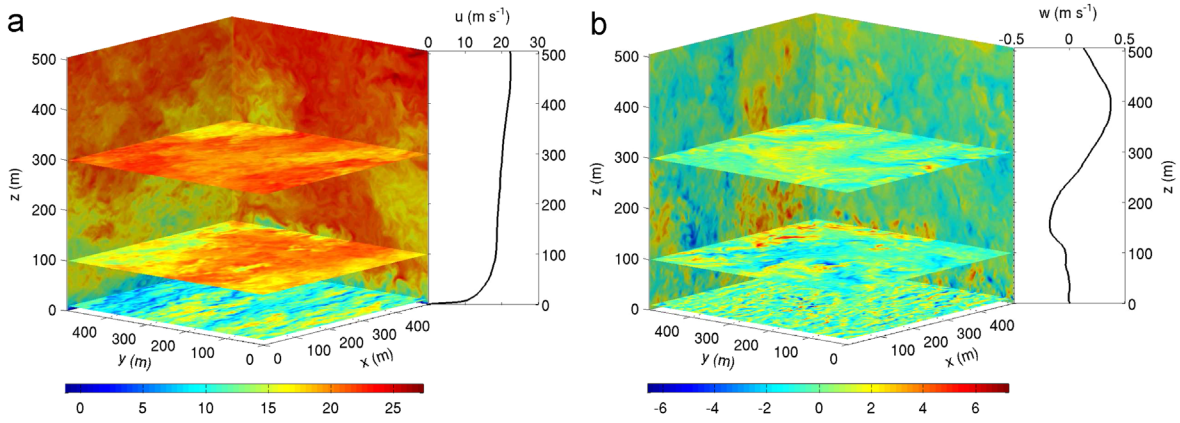

Fig. 2. Three-dimensional flow fields of the u- (a) and w- component (b) of the velocity. Wind speed contours in m s^{-1} are colored. Horizontal cross-sections at heights above ground of 10 m, 100 m and 300 m are slightly brighter colored in order to differ them from the vertical cross-sections.

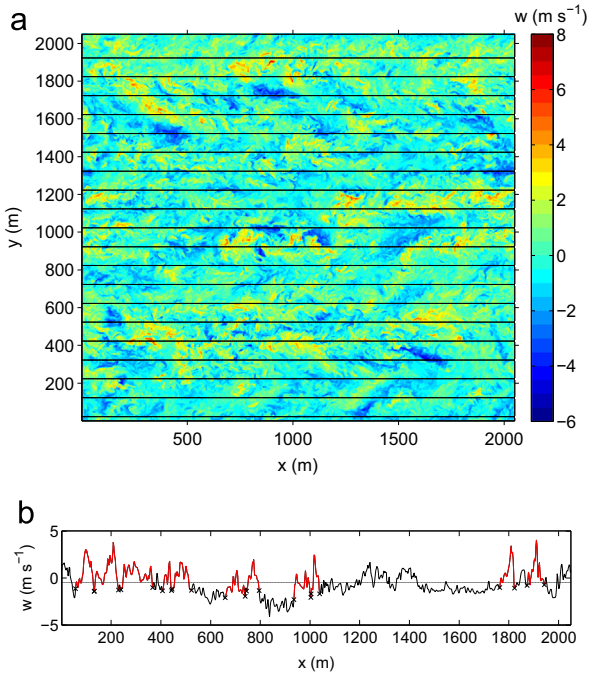

Fig. 3. Example of one-dimensional gust extraction from the horizontal cross-section of the vertical velocity component w at $z=100$ m after 1.5 h simulation time. In (a) the horizontal black lines indicate where the one-dimensional data were extracted from the instantaneous x–y plane. The velocity w obtained from the middle black line in (a) at $y=1020$ m is shown in (b). The discrete gusts fulfilling the gust criteria (see text) are marked in red. Crosses indicate the starting and end point of each gust. The mean wind speed of this measuring path is shown by the black line.

measurements of all three wind components were made. The paths are aligned parallel to the x-axis (in direction of the geostrophic wind vector), at regular intervals of 100 m. An example of these virtual measuring paths in one horizontal cross-section is shown in Fig. 3(a).

In previous investigations of one-dimensional gust characteristics, discrete gusts were often extracted from a turbulent wind signal by a peak-over-threshold method (e.g. Camp, 1968; Verheij et al., 1992). According to this method, the wind speed around a local maximum, which is equal or greater than the fixed threshold, is defined as gust. The beginning (starting point) and the end (end point) of the gust can be defined in different ways: one possibility is to define a certain time period (e.g. several seconds) around the maximum as total gust (see e.g. Bierbooms and Dragt, 1999). In this case, the maximum value coincides with the center of the gust and all gusts have the same duration. Another way is to define the intersection of the wind signal with the mean wind value as gust edges. The mean wind is typically the 10-minutes mean, or at least, a mean over the available measuring signal. A disadvantage of this method is that those parts of the gusts, which have lower values than the mean value, are cut off. This leads to a reduction of the total gust amplitude and the duration (or length). Furthermore, the missing wind speed data may contain important information about the velocity gradients at the edges of the gusts. For this reason, we used the local minima around the maximum value instead of a mean wind speed as definition for the gust edges. The two points where the wind speed signal crosses the larger value of the two minima are defined as starting and end point. Due to the discrete numerical grid, the two values of the beginning and end of the gust are generally not exactly equal. For this reason, we allowed a difference of 0.3 m s^{-1} (10% of the minimum amplitude $A_{\min}$) between these two values. An example of the application of the method described can be seen in Fig. 3(b). It shows the vertical velocity signal obtained from the virtual measuring path at $y=1020$ m in Fig. 3(a). The wind pulses fulfilling the gust criteria are marked in red. Their starting and end points are indicated by crosses. The gust criteria can be summarized as follows:

- The difference between the maximum value and the starting point (A_{min}) must be at least 3 m s^{-1}.
- The gust length is between 25 m and 150 m.
- The smallest value between the starting point and the gust end point is larger than the starting point value.
- The difference between the end point and the starting point is less than 10% of $A_{\min}$.

All red marked gusts cross the mean wind (horizontal black line). This points out the difference of the method used in the present study compared to those using the intersection of the instantaneous wind speed with the mean wind as gust edges.

After extracting the discrete gusts from the virtual measurements, they were classified according to their length. This classification is based on results of Camp (1968) and Verheij et al. (1992), who present in their studies dependencies of the gust shape on the duration. Intervals in steps of 25 m led to five gust classes between 25 m and 150 m. Within each interval, every gust was first normalized with its amplitude and length and then interpolated on a unique grid. At the end, a mean gust shape was calculated for each gust class.

The concept of calculating a mean gust shape was also already used in the studies of Camp (1968) and Verheij et al. (1992). On the one hand, specific information of some individual gusts may be averaged out, on the other hand, however, the most typical characteristics are emphasized. Thus, the calculated mean gusts represent typical gusts (which fulfill the above mentioned gust criteria) occurring in the turbulent wind field. The gust extraction method as described exemplary for the vertical wind component was applied in the same way on the data fields of the two horizontal velocity components. The corresponding mean gust shapes were calculated separately for u, v, and w. In contrast to the results obtained from mast measurements (e.g. Camp, 1968; Verheij et al., 1992) where only the magnitude of the horizontal wind speed was analyzed, our method provides gust shapes for each velocity component. Thus, the results contain information about the direction of the wind relatively to the virtual measuring path. However, it should be noted again that the direction of the virtual measuring path is the same for all wind components (along the x-axis). The results of all three wind components are shown in Chapter 4.

3.2. Two-dimensional gusts extraction method

The criteria used for the two-dimensional gust analysis are based on those of the one-dimensional gust analysis. Since the above criteria are not directly transferable to a two-dimensional gusts extraction algorithm, some modifications had to be implemented. An explanation of this algorithm will be given by means of Fig. 4. It illustrates the different steps of the procedure on a small section (150×150 m^2) of the vertical velocity field at a height of 30 m (Fig. 4(a)). In practice, the gust extraction algorithm was applied on the complete horizontal cross-section of each velocity component, height and point in time.

Due to the complex structures of the two-dimensional flow field, the method to detect the minima around the gust peak, as applied for one-dimensional gust extraction, could not be used. Instead, a constant value slightly above the mean was used to define the edge of each discrete gust. This value varies according to the wind component and the mean wind speed of the cross-section. It was chosen in such a way, that it is as close as possible

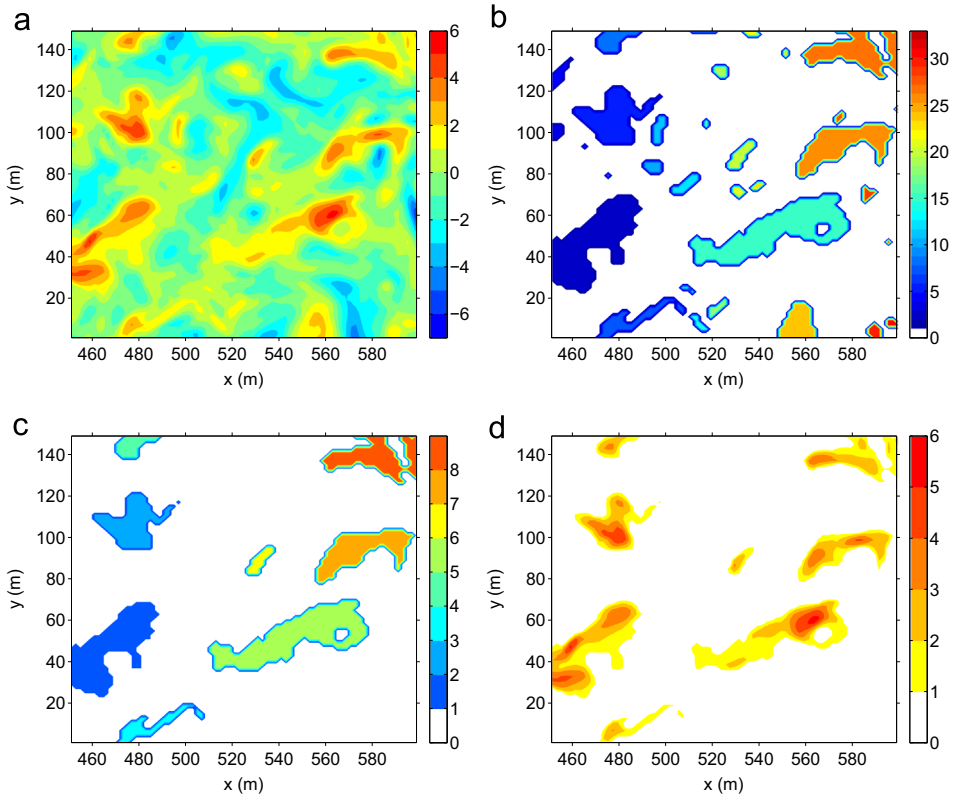

Fig. 4. Example of two-dimensional gust extraction method illustrated for a small horizontal section of the vertical velocity at $z=30$ m. In (a) the raw data of w in m s^{-1} are shown, (b) and (c) illustrate the numbered gusts before and after applying the gust criteria (see text), the final result of the extracted gusts in m s^{-1} is visible in (d).

to the mean wind speed one the one hand and the two-dimensional structures can still be distinguished from each other on the other hand. All wind speed values below this threshold were cut off from the data field. The remaining flow structures (or data objects) were detected and counted using the Matlab image processing toolbox function *bwlabel*. The result of this first step can be seen in Fig. 4(b). Each color represents one of the 32 detected objects in the shown area. In the next step the following gust criteria were applied:

- The minimum amplitude A_{min} relative to the mean wind speed is 3 m s^{-1}.
- The area representing a gust contains at least 10 grid volumes.
- The maximum diameter at the widest point of the gust is 150 m.

The mean wind speed was calculated as the average of the entire horizontal cross-section. In case of the vertical velocity it is zero for all heights (see also Fig. 1(c)). The resulting numbered objects (or gusts) fulfilling the above criteria are shown in Fig. 4(c). In this example, eight gusts remain from the original number of 32 objects of the previous step. In the final step, the corresponding wind speed values of the detected objects were determined (Fig. 4(d)).

During the analysis process of the two-dimensional gusts, it was found that the differences between the larger gust classes (50 m–150 m) are relatively small. In contrast, gust shapes of gusts with diameters smaller than 25 m show distinct differences compared to the larger gust shapes. For this reason, another gust classification than in the one-dimensional case is used for the two-dimensional gusts: The new three intervals with upper interval limits for the maximum diameter are 25 m, 50 m and 150 m. The lower limit of the first gust class is defined by the area of ten grid points which was applied as one of the above listed gust criteria.

Before calculating the mean gust shapes, each discrete gust was transferred to a unique two-dimensional grid and finally normalized with its amplitude and maximum diameter. A simple averaging of the two-dimensional gust data for each gust class led to nearly circular mean gust shapes. Since this would not reflect the typical gust shapes of the wind field as can be seen exemplary in Fig. 4 (most of the gusts are not circular, instead they have a rather elongated form), the discrete gusts were rotated in such a way, that their main axes were parallel to the x-axis. After the rotation, all gusts were averaged according to their gust class.

4. Results

In this section, the mean gust shapes of the one- and two dimensional gust analysis are presented. As mentioned above, gust shapes are normalized with the amplitude and length (or maximum diameter). The corresponding non-dimensional variables are marked with an asterisk (u^*, v^*, w^* for the velocity and x^* for the space scale). Due to the rotation of the two-dimensional gusts before the averaging, the resulting mean gusts are decoupled from the original horizontal coordinates x and y. The new space coordinates are orientated in direction of the axis of the elliptically shaped gusts and thus additionally marked with a subscribed ‘e’ (x_e^* and y_e^*).

One-dimensional gust shapes will primarily be compared with the one-cosine shape. Additionally, comparisons with measurements will be performed to verify the model data. The two-dimensional analysis provides information of the complete structure of gusts in the horizontal section. Both longitudinal and lateral gradients of the gust velocity can be obtained from the two-dimensional gust shapes.

For both types of gusts (one- and two-dimensional), analytical approximations are suggested and compared with the gust shapes obtained from the LES data. A discussion follows at the end of this chapter.

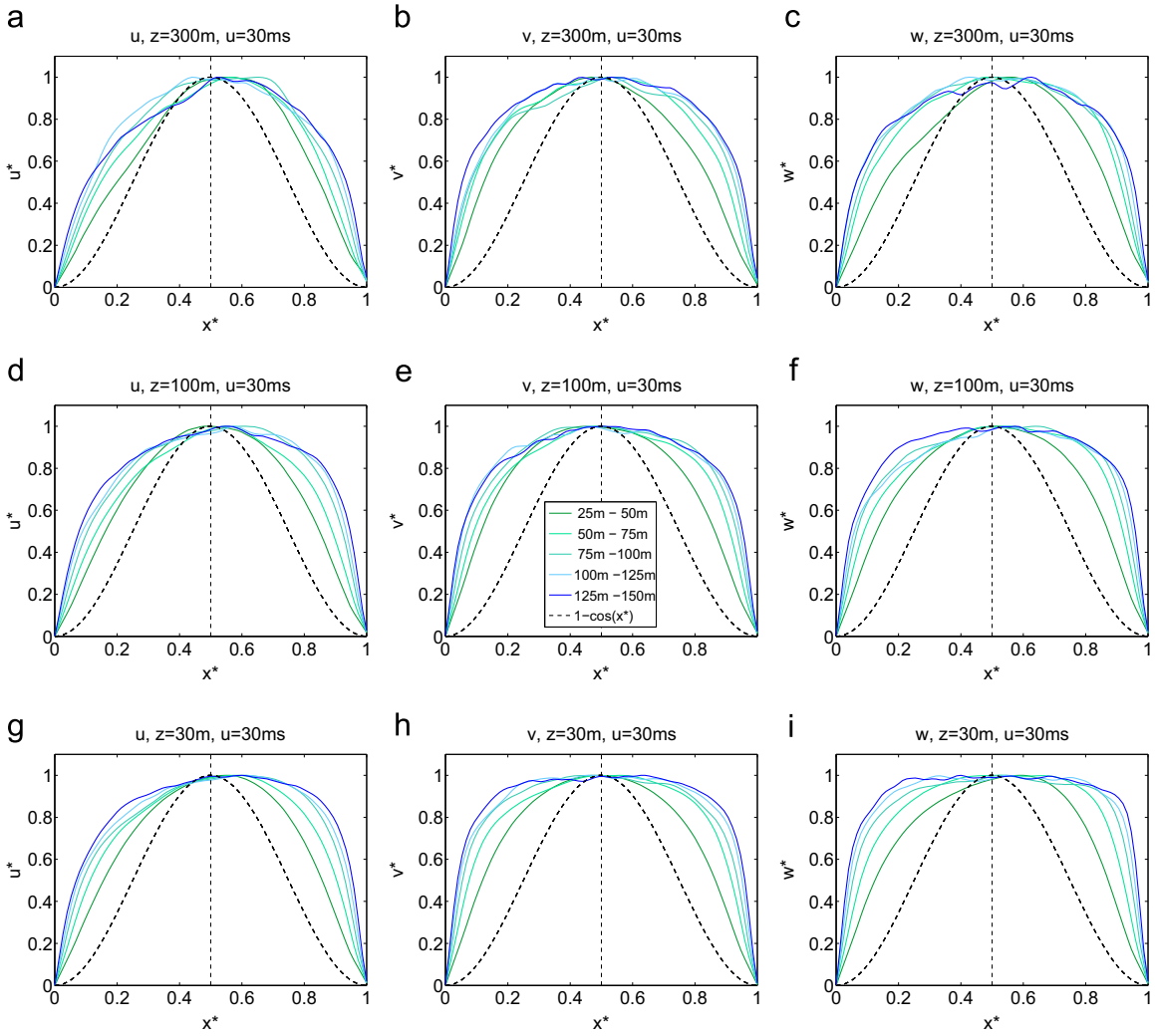

Fig. 5. Mean gust shapes of the three velocity components u^* (a), (d), (g), v^* (b), (e), (h) and w^* (c), (f), (i) at different heights of 30 m (g), (h), (i), 100 m (d), (e), (f), and 300 m (a), (b), (c). Additionally, the one-cosine gust shape is indicated by the black dashed line in each of the graphs. (For interpretation of the references to color in this figure caption, the reader is referred to the web version of this paper.)

4.1. One-dimensional mean gust shapes

4.1.1. Mean gust shapes obtained from LES

In order to achieve a meaningful statistics for the mean gust calculation, 24 instantaneous horizontal cross-sections were analyzed according to the gust extraction procedure describe above. Based on visual inspection, 50 discrete gusts were estimated as sufficient to obtain an adequate convergence in the mean gust shape. Only at the maximum analysis height of 500 m, the number of gusts of each gust class is below this value. At the lowest height levels (below 100 m), more than 500 gusts of each velocity component and gust class were extracted and averaged.

Fig. 5 shows the mean gust shapes calculated for the three velocity components u^*, v^*, and w^* (from left to right) in three heights 30 m, 100 m, and 300 m (from bottom to top). The dashed curves in the figure represent the one-cosine gust. For a better orientation and to further emphasize asymmetries, the middle of the x^*-axis is marked with a dashed vertical line. In comparison with the smaller gusts, larger gust shapes tend to have a larger spatial extend in the upper part which is partly constant. A steeper increase and decrease at the edges occurs for the larger gusts. These differences between the gust classes are visible in all graphs of Fig. 5. It is most pronounced in the gust shapes of the vertical velocity at $z=30$ m (Fig. 5(i)). Approximately 80% of the largest mean gust in this graph (dark blue curve) consists of the constant middle part. Starting from this rather trapezoidal curves, gust shapes become a much more rounded form by going to greater heights. A similar change in gust shapes is visible by taking the three velocity components at the same height into account. Vertical gust shapes are wider in the upper part than horizontal gusts, with gusts of the v-component being the wider of the horizontal components. In some gust shapes, a slight asymmetry can be seen, especially in the u-component (see e.g. Fig. 5(g)). The maximum of these curves is shifted to the right and, hence, the slope on this side is steeper than on the left side. Transferring these gust shapes to the wind field where the data are obtained from, it means that a fixed observer or a measuring system would feel or record first the steeper part of an arriving gust. This fact becomes clear, when the gusts of Fig. 5 are seen as static wind pulses which are transported with the surrounding flow in the direction of the positive u-component (in x^*-direction) from left to the right. The differences in the slope of rise and decay could also be observed in the horizontal velocity of mast measurements (Camp, 1968) and will be discussed in detail at the end of this chapter.

The comparisons of the gust shapes obtained from the LES and the one-cosine law in Fig. 5 show distinct differences. The largest differences in the curves are visible in the lowest altitudes for the longest gusts. However, even the distance between the nearest

curve of the mean gust from LES and the one-cosine gust shape (in greater heights, e.g. green and dashed black line Fig. 5(a)) is approximately of the same magnitude than the distance between the curve of the smallest gust class and the largest gust class.

4.1.2. Analytical description of the mean gust shapes

In aircraft design processes, discrete gusts are described by the one-cosine law (FAR, 2012). As pointed out in the above section, the results obtained from LES predominately show distinct differences to this classical gust shape. For this reason, we suggest an analytical approach which differs from this classical gust shape approximation. Requirements for this approach are to be held rather simple and practicable for potential users. On the other hand, it should adequately describe the main features of the mean gusts presented in the previous section like the steep increase and decrease, the partly constant middle part as well as their height dependence and differences between the velocity components and gust classes.

Since the gust shapes obtained from the LES agree better with those obtained from mast measurements of Camp (1968) than with the one-cosine law, our approach is based on the analytical function describing the horizontal gusts of the study from Camp (see Jones, 1971; Frost et al., 1978). The modified gust shape is

$$U(x^*) = 1.58(1 - \exp(-\sin(\pi x^*)^k)), \tag{2}$$

with k as a gust length depending dimensionless parameter which can be written as

$$k = \frac{1}{k_h L}, \tag{3}$$

where L is the length of the gust in meters and k_h (in m^{-1}) is calculated as

$$k_h = k_U + \frac{1}{50 \ln\left(z \cdot \frac{1}{\mathrm{m}}\right)} \cdot \frac{1}{\mathrm{m}}. \tag{4}$$

The velocity $U(x^*)$ in Eq. (2) represents the three velocity components u^*, v^* and w^* which depend on the normalized stream-wise coordinate x^*. The coefficient k_U varies depending on the wind component. It takes the values of $0.008\ \mathrm{m}^{-1}$, $0.014\ \mathrm{m}^{-1}$ and $0.016\ \mathrm{m}^{-1}$, respectively for the velocity components u^*, v^* and w^*. In contrast to the approach of Jones (1971), no asymmetry is considered in Eq. (2). The reason for this is that the asymmetry is less pronounced than in the results of Camp (1968) and primarily visible in the u-component. First attempts to consider the asymmetry in the analytical approximation did not show a significant improvement compared to Eq. (2).

A comparison of the analytical approach and the virtually measured gust shapes can be seen in Fig. 6. For a better clarity, only the largest and smallest gust class at heights of 30 m and 100 m of the u^*- and w^*-components are shown. These mean gust shapes clearly show all characteristics pointed out in Section 4.1.1. The analytical gust shapes agree well with the gust shapes obtained from the LES data. As already mentioned above, the asymmetry, primarily visible in Fig. 6(c), could not be reproduced. Furthermore, the trapezoidal vertical gust shapes of the larger gust class (Fig. 6(d), blue line) are slightly smoother at the upper edges of the constant middle part in case of the analytical approximation. Despite these differences, the suggested analytical gust shapes agree considerably better than the one-cosine gust shape indicated by the dashed black line in all graphs of Fig. 6.

Not illustrated here are the results of the other height levels and the horizontal velocity component v^*. They also show a good agreement between the virtually measured mean gust shapes and

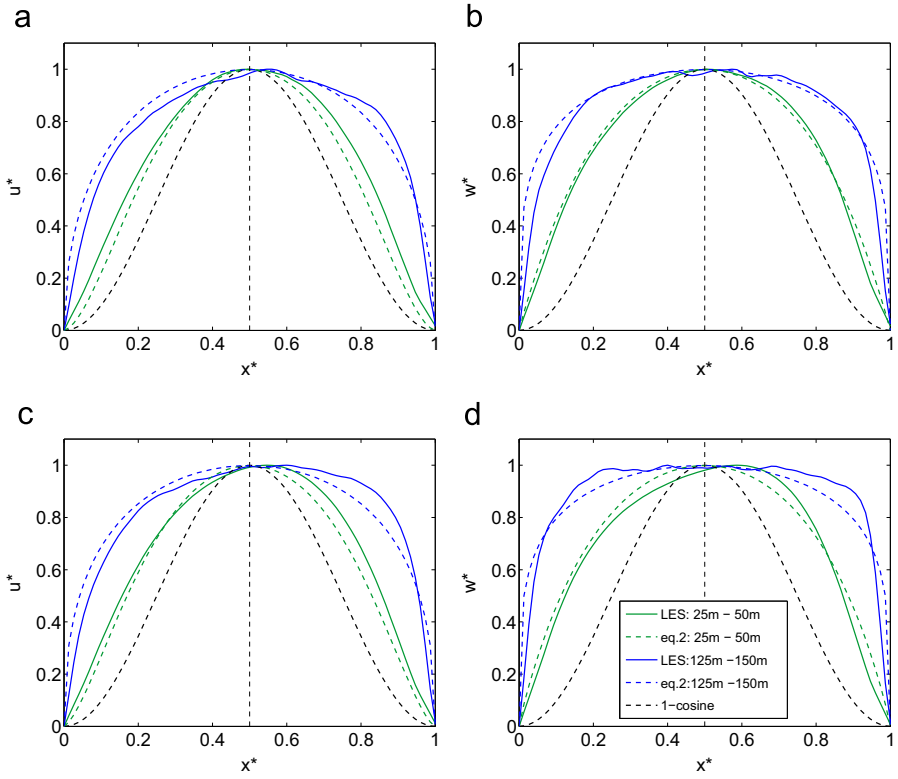

Fig. 6. Comparison of mean gust shapes of the largest and smallest gust classes obtained from LES (solid lines) and analytical approximation using Eq. (2) (dashed lines) of the velocity components u^* (a), (c) and w^* (b), (d) at different heights 30 m (c), (d) and 100 m (a), (b). The one-cosine gust shape is shown as dashed black line. (For interpretation of the references to color in this figure caption, the reader is referred to the web version of this paper.)

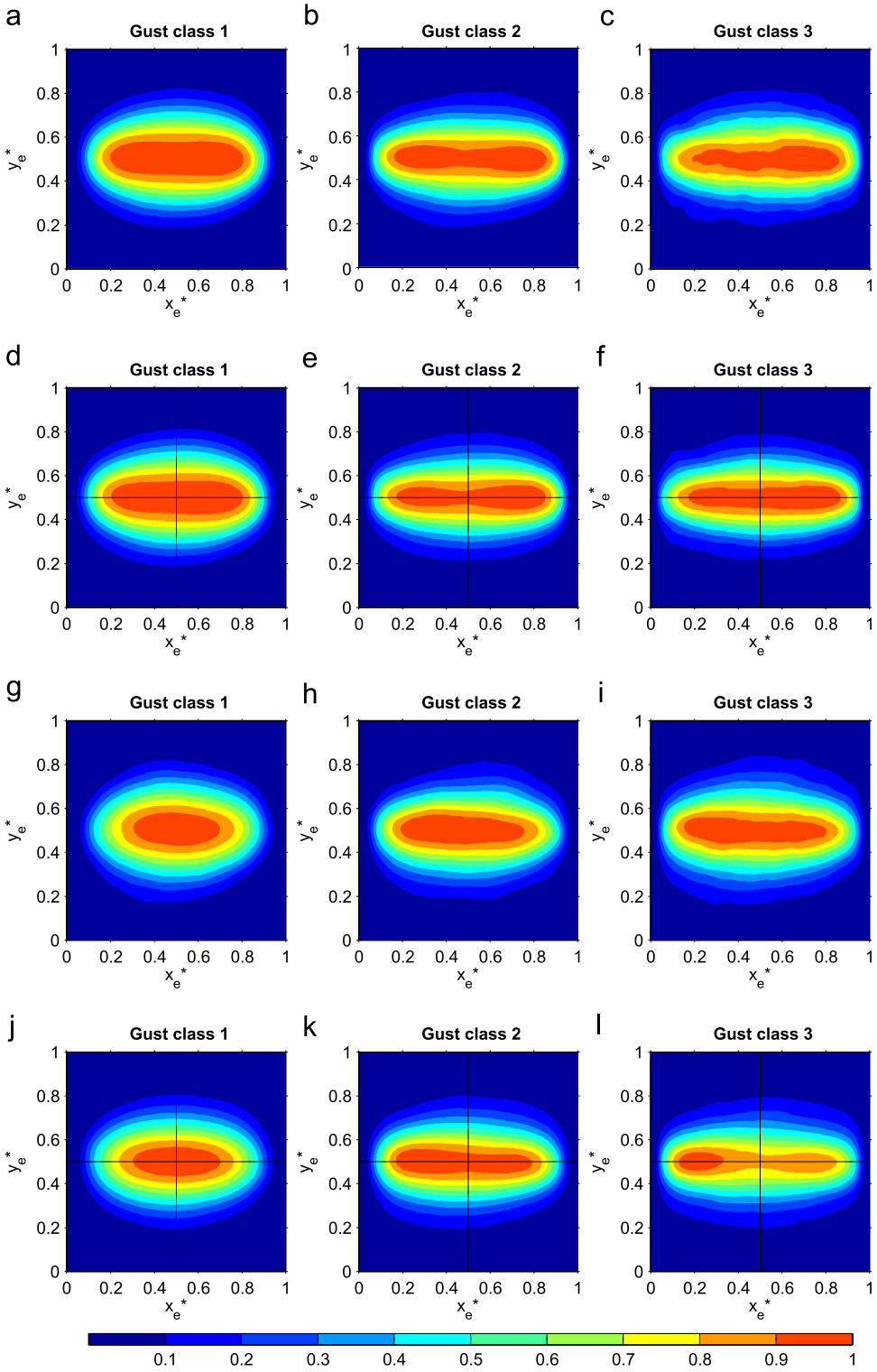

Fig. 7. Mean two-dimensional gust shapes of the normalized velocity components u^* (a)–(f) and w^* (g)–(l) at two different heights of 30 m (d)–(f), (j)–(l) and 100 m (a)–(c), (g)–(i). Black lines in (d)–(f) and (j)–(l) indicate the data extraction paths for Fig. 8.

the corresponding analytical approximation. However, it should be pointed out, that the consistence is less for higher altitudes. Due to the smaller number of extracted gusts, the mean gust shapes are less smooth and differ more from the analytical approach than those of the lower altitudes.

4.2. Two-dimensional mean gust shapes

4.2.1. Mean gust shapes obtained from LES

The procedure, as described in Section 3.2 for a small part of the flow field, was applied on the complete horizontal section for

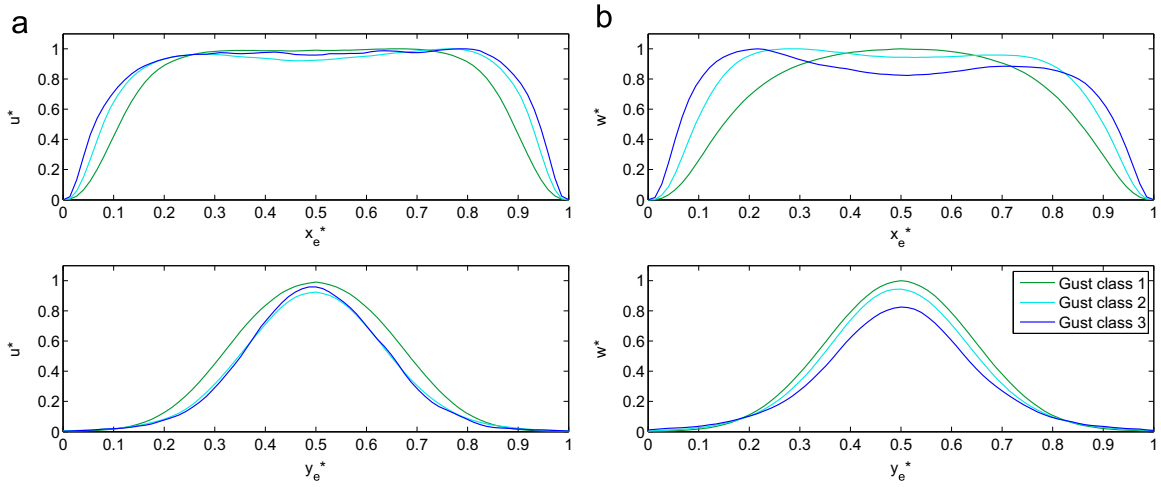

Fig. 8. Mean gust shapes of the velocity components u^* (a) and w^* (b) along the major axis (parallel to x^*-axis) and along the minor axis (parallel to y^*-axis) of the two-dimensional gust shapes at a height of 30 m. The corresponding two-dimensional gust shapes are Fig. 7(d)–(f) for (a) and Fig. 7(j)–(l) for (b). (For interpretation of the references to color in this figure caption, the reader is referred to the web version of this paper.)

each point in time and height level. Each velocity component was analyzed separately. It should be noted again, that the mean two-dimensional gust shapes were divided in three classes (in contrast to five in the one-dimensional case).

Fig. 7 shows the results of the mean gust shapes of the two wind components u^* and w^* at 30 m and 100 m height. Mean gust shapes of the horizontal velocity component v^* are not illustrated, because they hardly differ from the u^*-component gust shapes. The main characteristics of all mean gusts in Fig. 7 are their elliptically shaped contours. For larger gusts, the aspect ratio becomes larger. This fact is more pronounced at the lower heights of both velocity components and can bee seen more clearly in Fig. 8, where the gust shapes along the major and minor axes are shown for an altitude of 30 m. The corresponding paths along which the data were extracted are indicated in Fig. 7 by the black lines. For both velocity components, the gust shape curves become longer in x_e^*−direction (along the major axis) for larger gusts. In contrast, they become more narrow along the minor axis for larger gusts. Qualitatively, the one-dimensional wind speed data along the major axis of the ellipses agree with the one-dimensional gust shapes analysis presented in Section 4.1.1. Longer gusts have a rather trapezoidal shape, whereas smaller gusts are closer to the one-cosine shape. Due to the different methods of extracting the discrete gusts, the results shown in Fig. 8 are not quantitatively comparable with the one-dimensional gust shapes in Fig. 5. The main difference of the methods is the rotation of the two-dimensional gust shapes before averaging them, which leads to a decoupling of the coordinate system. The original position of each discrete two-dimensional gust cannot be reconstructed, whereas the one-dimensional gust shapes are orientated in direction of the x-coordinate.

A further characteristic of the two-dimensional mean gusts shapes, which can be seen in Fig. 8 (and also partly in Fig. 7), is the local minimum at the center of the gusts of gust classes 2 and 3. The maxima are located at the edges of the gusts on the major axis. The largest difference between the centered minimum and the larger of the surrounding maxima is visible in the gust shape representing the largest gust class of the vertical velocity at 30 m height and reaches nearly 20% of the maximum gust strength (blue curve in Fig. 8(b)). In this case, an asymmetry is also visible. The left local maximum reaches larger wind speed values than the right local maximum (see also Fig. 7(l)). Since this characteristic (local minimum in the gust center) does not exist in the results of the one-dimensional gust shape analysis, it might be caused by the differences in the analysis methods. However, the physical explanation for the local extrema can be given by the superposition of several turbulent eddies (or wind speed peaks) within each discrete gust. This can exemplary be seen in Fig. 4, where each of the larger gusts has several local maxima which may also be denoted as 'subgusts'. In case of the larger two-dimensional gusts, these local maxima of the discrete gusts seem to be located preferably at the edges of the gusts, which lead to the mean gust shapes shown above. Since the focus of the present study lies on mean gust shapes, a detailed analysis of the internal structure of each discrete gust was not performed.

Variations of the mean gust shapes with height above ground are very small. Above $z=100$ m, nearly no differences between the gust shapes within the same classes are visible. Below this height, the aspect ratios of the gust shapes of all wind components and classes tend to become slightly larger by reducing the height (best visible in the shapes of the smallest gust class in Fig. 7). The largest differences occur between the lowest analyzed heights of 10 m and 30 m above ground (not shown here).

4.2.2. Analytical description of the mean gust shapes

Based on the two-dimensional mean gust shapes presented in Section 4.2.1, we derived an analytical two-dimensional gust model. No currently existing discrete two-dimensional gust models based on mean gust shape analysis obtained form field measurements or turbulence resolving numerical simulations are known to the authors. For this reason, the new gust model allows much more complex analysis in aircraft or structure design processes in future.

The approach to derive the two-dimensional gust model is based on the one-dimensional expression (see Eq. (2)). That means that the combination of the exponential and sine function is expanded by the second space dimension y_e^* and is modified in that way that it reproduces the above results. The new formula reads as follows:

$$U_{2D}(x_e^*,y_e^*) = k_7 \cdot [1-\exp(-((\sin(\pi \cdot (\tanh(k_5 \cdot (k_6 \cdot (x_e^*-0.5)^2+1) \cdot (y_e^*-0.5))+1)/2)^{k_2}) \cdot (\sin(x_e^* \cdot \pi)^{k_1})))] \cdot (k_4 - \sin(x_e^* \cdot \pi)^{k_3}), \quad (5)$$

The first and second sine functions represent the gust shapes in the two space directions (comparable to the one-dimensional formula). In the y_e^*-direction, the sine function is modified by the

hyperbolic tangent which leads to a reduction of the values of U_{2D} (respectively u^*, v^* and w^*) at the edges of the gust in the direction of x_e^*. Without this expression, the gust shape contours would be rather rectangular instead of elliptical. The third sine function modifies the constant middle part of the gust. It allows a local minimum in the center of the gust.

Due to the complexity of the two-dimensional mean gust shapes, a set of seven coefficients for each gust shape would be necessary to describe all different mean gust shapes obtained from the LES analysis. Considering all wind components, gust classes, and altitudes, this would led to more than 400 coefficients and make future applications of the proposed gust model rather inconvenient. Thus, we decided to neglect the differences of the gust shapes with height and between the two horizontal wind components. Since these differences are not very pronounced (see section above), the gust shapes obtained with the chosen set of components for Eq. (5) lead to gust shapes representing all gusts with a sufficient accuracy. The typical characteristics as the differences between the vertical and horizontal wind components and the differences between the gust classes are considered. The chosen coefficients are listed in Table 1.

Two examples of a comparison of the mean gust shapes obtained from the LES and the gust model (Eq. (5)) can be seen in Figs. 9 and 10. They show the mean gust shapes of the vertical velocity at a height of 30 m of which the LES mean gust shapes were already shown in Fig. 7. The smallest gust class 1 and the largest gust class 3 of w^* are chosen, because they differ considerably from the other and the typical characteristics of the corresponding gust class become evident. Thus, both strengths and weaknesses of the two-dimensional mean gust model can be clearly pointed out. Fig. 9 shows the comparison of gust class 1. Almost no difference is visible in the contour lines of the velocity. The wind speeds along the major and minor axes show that the increase and decrease along the axis of the ellipse are very well reproduced.

Fig. 10 shows the comparison of gust class 3 for the vertical wind component at 30 m height. In this case, small differences in the contour lines are visible. In the LES gust shape, two local maxima appear. They are both visible in the contour plot and the velocity curve along the major axis below (blue curve). The maximum on the left side which is also the absolute maximum, is nearly 12% larger than the second maximum on the right side. Since the analytical function only produces symmetrical gusts, this characteristic cannot be reproduced by the gust model. However, the double-shaped form is well reflected. Due to the curve fitting approach used, the velocity values of the two local maxima of the analytical mean gust shape lie approximately between the two values of the LES gust shape maxima. The local minimum at the gust center is well reproduced, which can also be seen in the velocity curves along the minor axis (Fig. 10, below). As in Fig. 9, the increasing and decreasing parts of the analytical gust shapes along both elliptical axes agree well with the LES gust shapes.

Other two-dimensional LES mean gust shapes typically show a smaller degree of asymmetry (see e.g. Fig. 7), than the vertical gust shape illustrated in Fig. 10. Thus, the proposed analytical approximation has a greater agreement with the corresponding mean gust shapes obtained from LES than those presented in Fig. 10. Only at heights of 300 m and above, the differences between the analytical and the LES mean gust shapes become significantly larger because the number of detected gusts is not sufficient to obtain smooth mean gust shapes. However, the main characteristics, like the diameter and the aspect ratio can clearly be observed in these gust shapes and thus also be reproduced by the gust model.

Table 1
Coefficients k_i to reproduce the two-dimensional gust shapes using Eq. (5).

Wind component	Gust class	k_1	k_2	k_3	k_4	k_5	k_6	k_7
u*,v*	1	1.9	4.6	0.12	1.08	2.3	2.0	19.2
	2, 3	1.2	1.4	0.2	1.2	5.4	1.5	7.7
w*	1	1.5	1.3	3.0	5.0	5.0	1.0	0.395
	2	1.5	1.4	0.2	1.18	5.1	1.1	8.5
	3	1.3	1.1	0.1	1.07	6.0	1.2	19.0

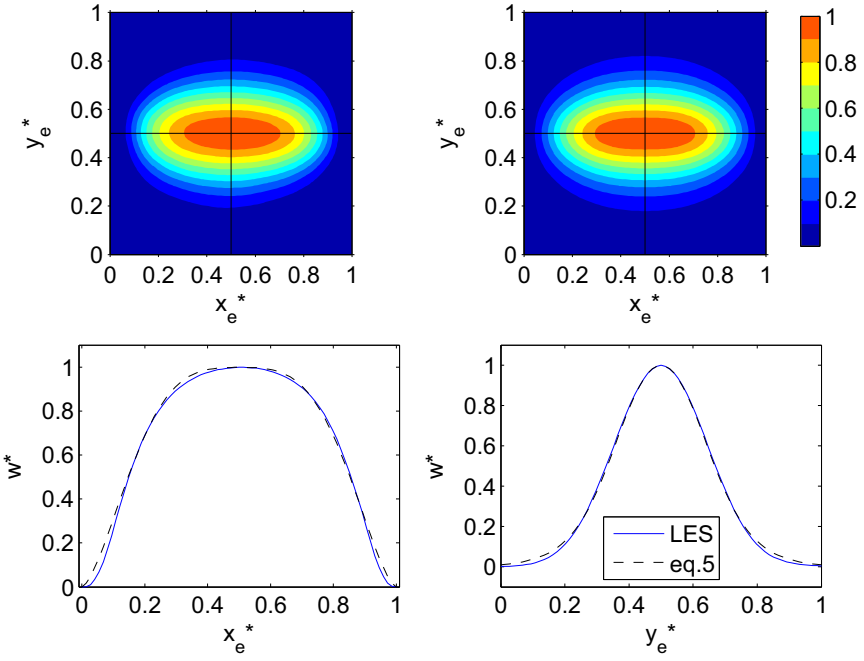

Fig. 9. Comparison of the two-dimensional mean gust shapes of class 1 obtained from LES (upper left) and Eq. (5) (upper right) of the velocity component w^* at a height of 30 m. Corresponding velocities along the major and minor axes are shown below.

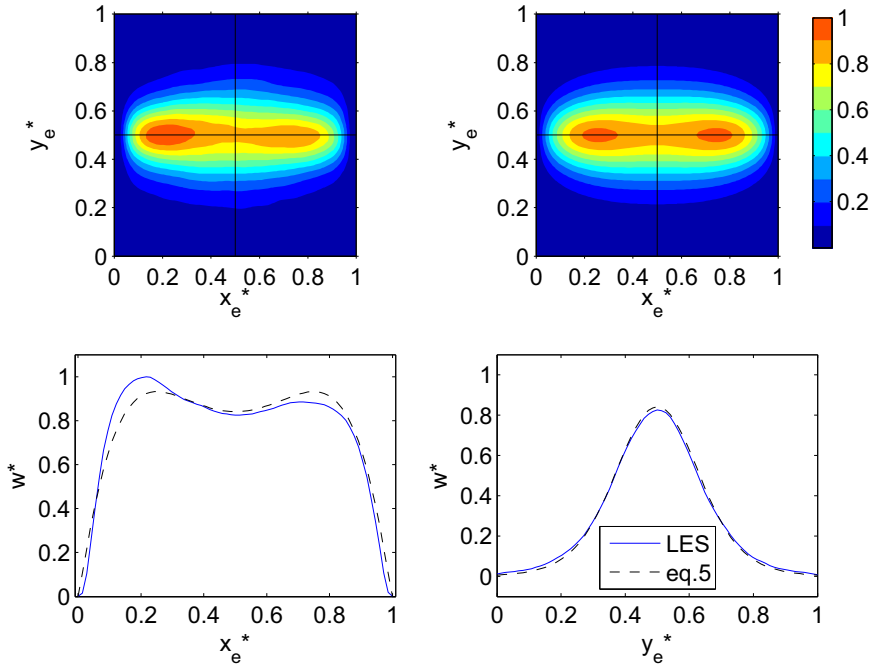

Fig. 10. As Fig. 9 but for gust class 3. (For interpretation of the references to color in this figure caption, the reader is referred to the web version of this paper.)

4.3. Discussion

The results of the mean one-dimensional gust shapes obtained from LES show significant differences compared to the one-cosine law. Especially gusts of the larger classes deviate distinctly from the classical shape. In contrast, the main characteristics of the gusts (steep increase and decrease with rather constant middle part) qualitatively agree with the results obtained from mast measurements of Camp (1968) and Verheij et al. (1992). More recent gust shape calculations from Bierbooms and Dragt (1999) indicate a rather sharp peak shaped mean gust. In their mast measurement analysis, Bierbooms and Drag centered the maximum value of each discrete gust and used a constant time period of one minute around this extreme value for the ensemble average. Thus, the starting and end point of the discrete gusts depend only on the time scale, not on the wind speed value. A classification to a different gust duration (respective length) was not done. Assuming the frozen turbulence theory and the mean wind speed value mentioned in Bierbooms and Dragt (1999), the mean gust length would be 600 m which is four times the maximum gust length of our investigations. It is obvious, that this method of Bierbooms and Drag leads to different results than the method used in the present study or used by Camp (1968) and Verheij et al. (1992).

Differences in the presented results of the one-dimensional analysis concerning the three wind components are mainly visible in the variable length of the constant middle part of the gust shapes. It is not possible to validate this characteristic by means of the mast measurements mentioned above, because they only consider the magnitude of the horizontal wind speed.

A slight asymmetry could be seen in the u^*-component of the one-dimensional analysis. On this aspect, mast measurements do not provide unique results. Camp (1968) observed in his measurements a stronger inclination of the gust shapes than the LES gust shapes show (in the u^*-component). The direction of the displacement of the gust maximum, however, is the same. Verheij et al. (1992) in contrast summarize the gust shapes obtained from his mast measurements as symmetrical. Reasons for these differences may be the different meteorological conditions both during the measuring campaigns and the numerical simulation. In the presented LES study, only one specific meteorological scenario (a strong wind event) was analyzed. The field experiments, however, contain wind speed data of various weather situations occurring over a long time period. Weather situations like weak mean wind situations as well as convective boundary layer conditions may occur during the measurements. Furthermore, different analysis methods were applied (e.g. different values of A_{min} and different definitions of gust edges were used). Despite these differences, the main characteristics of the one-dimensional gust shapes obtained from LES qualitatively agree with those of the mast measurements from Camp (1968) and Verheij et al. (1992). Furthermore, the presented results provide gust shapes of all wind components independently of each other. Especially the vertical wind component was not considered in the previous analysis mentioned above and may provide important information for calculations during aircraft and wind turbine design processes.

Due to the differences between the LES mean gust shapes and the one-cosine law pointed out above, an analytical approach describing the LES gust shapes is suggested. It reproduces the one-dimensional mean gust shapes very well. The gust model is based on the approach described by Frost et al. (1978) and adjusted to the observed LES gusts. Besides the dependence on space (instead on time), the presented function considers the rather symmetrical shape of the gusts and reproduces the typical gust characteristics that depended on height for all defined gust classes of the three wind components u^*, v^* and w^*. However, the model is kept relatively simple to be comfortably implementable in future studies. A higher accuracy could only be achieved at the expense of its simplicity.

A validation of the two-dimensional mean gust shapes obtained from LES by means of field measurements is currently not possible because of a lack of high-resolution data and gust studies. Due to the agreement of the one-dimensional mean gust shapes from LES with results from mast measurements on the one hand and the consistent method (same database, same gust extraction method as far as possible) used for the one- and two-dimensional analyses in the presented study on the other hand, it seems to be reasonable to assume that the two-dimensional results are meaningful. This

assumption is supported by the agreement of the shapes along the axis of the ellipses of the two-dimensional mean gusts with the shapes of the one-dimensional analysis.

As in the one-dimensional case, an analytical approximation of the mean two-dimensional gust shapes is suggested. The formulation is much more complex than the one-dimensional gust model, since it contains mutual dependencies of the two horizontal space directions and a set of seven coefficients to describe the mean gust shape. However, the gust model is held as simple as possible to be applicable in further studies. The comparison of gust shapes shows a very good agreement between the analytically calculated gust shapes and the mean gust shapes obtained from LES.

The suggested two-dimensional mean gust shape model reproduces the typical characteristics like the elliptically shaped contours, the steep increase and decrease as well as the constant middle part respectively the double-shaped maxima of the larger gusts. The provided coefficient vectors allow to calculate the mean gust shapes depending on the velocity component and the gust classes. The altitude is not considered in the mean two-dimensional gust shape model since the analyzed LES gust shape variations are very small with height above ground.

The information provided by the two-dimensional approach can help to improve calculations of gust interaction with structures like aircraft and wind turbines. An aircraft traversing the same two-dimensional gust by various angles relatively to the major axis may presumably react differently on the wind induced forces. The same situation is conceivable for an earth-fixed structure like a wind turbine interacting with an advected gust. It is also very likely that a two-dimensional gust shape which is uniform over the complete width of the structure would cause different loads since lateral velocity gradients are missing. Further studies are necessary to quantify these differences and, hence, the possible advantages of the two-dimensional gust model over the currently used one-dimensional approaches.

The present study focused on the analysis and analytical approximation of mean one- and two-dimensional gust shapes. The suggested discrete mean gust models represent the typical characteristics of discrete gusts extracted from the LES flow fields. However, due to the complexity of turbulence and, hence, of gusts on the one hand and 'smoothing' of the shapes during the averaging process, they do not necessarily represent all types of discrete gusts occurring in a turbulent flow. Furthermore, the flow field may contain severe wind pulses which do not meet the gust definition criteria used in the present study like a sharp increase of the wind speed without a direct reduction to the initial value. These more detailed analyses of each discrete gust will be the subject of future investigations.

5. Summary and conclusions

Mean one- and two-dimensional gust shapes were calculated and analytically approximated by means of LES data. A high resolution simulation representing the turbulent lower part of an idealized strong-wind event caused by low-pressure system was performed. Virtual measurements of all three wind components in instantaneous cross-sections at different heights provided a sufficient amount of wind data for the statistical analysis. Both one- and two-dimensional gusts were extracted from the same wind fields using specific criteria for the gust amplitude, and length or diameter. All discrete gusts were classified corresponding to their length as well as scaled in space and strength. At the end, a mean gust shape for each gust class and velocity component was calculated.

Results of the mean one-dimensional gust shape calculations show a steep increase and decrease of the wind speed with a rather constant middle part. The spatial extension of this constant part varies depending on the wind component, the gust class, and the height above ground at which the gust was observed. In lower height levels, it reaches up to 80% of the total gust length for the gust shape of the vertical velocity component. This is a major difference in comparison to the classical one-cosine gust shape which has smaller spatial extend in the upper part and a shallower increase and decrease of the wind speed than all gust shapes calculated from the LES data. In contrast, gust shapes obtained from different mast measurements of previous studies, which are based on a similar gust extraction method, qualitatively agree well with the presented results. The suggested mathematical approach reproduces the typical characteristics observed in the one-dimensional LES results for each wind component, gust class, and height level.

The analysis of two-dimensional mean gust shapes show elliptical contours for all gust classes of all wind components and heights. As in the one-dimensional case, the larger gusts tend to have a longer constant middle part along the major axis and hence a larger aspect ratio than the smaller gusts. Similarly, the mean gust shapes vary with height. The largest aspect ratio in each gust class for each velocity component appears for the lowest investigated height level of 10 m. Mean gust shapes of higher altitudes have a larger spatial extend in direction of the minor-axis and, hence, have a smaller aspect ratio.

Based on the analytical approximation for the one-dimensional gust shapes, a two-dimensional approach has been suggested. It contains a set of seven coefficients in order to consider the typical characteristics observed in the analysis.

The proposed coefficient vectors allow to reproduce the mean gust shapes considering the different velocity components and gust classes. A good agreement between the LES mean gust shapes and the two-dimensional mean gust shapes calculated with the proposed gust model is shown.

The results presented in this study were obtained from a large-eddy simulation of a strong-wind weather situation associated with a low-pressure system. A geostrophical wind velocity of $30\ \mathrm{m\,s^{-1}}$ was used to generate strong wind shear and turbulence. Nevertheless, the calculated mean gust shapes are representative for similar meteorological situations with different strengths of background wind. This follows from the fact, that the physical processes leading to the turbulence and gusts (in this case wind shear) are identical for all high Reynolds number flows among which also the presented meteorological situation classifies. Large variations of the geostrophical wind, e.g. a reduction to less than $10\ \mathrm{m\,s^{-1}}$ would require a modification of the gust extraction criteria (e.g. another A_{min} must be used) which might result in a modification of the results. This is also the case, if the other meteorological conditions are basically changed. Severe turbulence caused by strong convection and downbursts associated with thunderstorms or frontal systems, for example, may contain gusts with significantly different characteristics. Since these meteorological phenomena are isolated storm events with a limited spatial and temporal extension compared to a stormy low-pressure system, this kind of weather phenomena was not considered in the present study.

Besides studying further different meteorological scenarios, the focus of the future work lies on a detailed analysis of the most extreme discrete gusts. Due to the averaging process applied in the present study, no statement on the strongest total wind speeds or the strongest velocity gradients occurred can be given. The knowledge of the frequency of occurrence as well as the corresponding velocity gradients of such extreme events may help to further improve the discrete gust models.

Acknowledgment

This work has been carried out within the research group FOR 1066 (http://www.for1066.tu-bs.de/) and was founded by the German Research Foundation (DFG) grant RA 617/19-2. Numerical simulations have been carried out on the SGI-ICE system of the North-German Supercomputing Alliance (HLRN).

References

Andersson, E., Häggström, J., Sima, M., Stichel, S., 2004. Assessment of train-overturning risk due to strong cross-winds. J. Rail Rapid Transit 218, 213–223.

Arakawa, A., Lamb, V.R., 1977. Computational design of the basic dynamical processes of the UCLA general circulation model. In: Chang, J. (Ed.), General Circulation Models of the Atmosphere, Methods in Computational Physics, vol. 17. Academic Press, Berlin, pp. 173–265.

Bierbooms, W., Dragt, J.B., 1999. Verification of the mean shape of extreme gusts. Wind Energy 2, 137–150.

Born, K., Ludwig, P., Pinto, J.G., 2012. Wind gust estimation for Mid-European winter storms: towards a probabilistic view. Tellus A 64, 17471.

Burton, T., Jenkins, N., Sharpe, D., Bossanyi, E., 2011. Wind Energy Handbook, second ed. John Wiley & Sons, Chichester.

Camp, D.W., 1968. Wind velocity measurements of low level wind gust amplitude and duration and statistical gust shape characteristics. Natl. Aeronaut. Space Adm. Tech. Memo.

Deardorff, J.W., 1980. Stratocumulus-capped mixed layers derived from a three-dimensional model. Bound.-Layer Meteorol. 18, 495–527.

Drobinski, P., Foster, R., 2003. On the origin of near-surface streaks in the neutrally-stratified planetary boundary layer. Bound. Layer Meteorol. 108, 247–256.

Federal Aviation Regulations: Part 25 – Airworthiness Standards: Transport Category Airplanes. Department of Transportation, Federal Aviation Administration, Washington, DC.

Friderichs, P., Göber, M., Bentzien, S., Lenz, A., Krampitz, R., 2009. A probabilistic analysis of wind gusts using extreme value statistics. Meteorol. Z. 18, 615–629.

Frost W., Long B.H., Turner, R.E., 1978. Engineering Handbook on the Atmospheric Environmental Guidelines for Use in Wind Turbine Generator Development. National Aeronautics and Space Administration, Technical Paper 1359.

Harlow, F.H., Welch, J.E., 1965. Numerical calculation of time-dependent viscous incompressible flow with free surface. Phys. Fluids 8, 2182–2189.

Hau, E., 2006. Wind Turbines, second ed. Springer-Verlag, Berlin, Heidelberg, p. 783.

Hoblit, M., 1988. Gust Loads on Aircraft: Concepts and Application. American Institute of Aeronautics and Astronautics, Washington D.C.

Jones, J.G., 1971. A unified discrete gust and power spectrum treatment of atmospheric turbulence. In: RAeS/AIAA/CASI Conference on Atmospheric Turbulence, London.

Kristensen, M., Casanova, M.S., Troen, I., 1991. In search of a gust definition. Bound.-Layer Meteorol. 55, 91–107.

Letzel, M.O., Krane, M., Raasch, S., 2008. High resolution urban large-eddy simulation studies from street canyon to neighbourhood scale. Atmos. Environ. 42, 8770–8784.

Mason, P.J., Thomson, D.J., 1987. Large-eddy simulations of the neutral-static-stability planetary boundary layer. Q. J. R. Meteorol. Soc. 113, 413–443.

Pratt, K.G., Walker, W.G., 1954. A Revised Gust-Load Formula and A Re-Evaluation of V-G Data Taken on Civil Transport Airplanes From 1933 to 1950. NACA TR-1206.

Raasch, S., Etling, D., 1998. Modeling deep ocean convection: large eddy simulation in comparison with laboratory experiments. J. Phys. Oceanogr. 28, 1786–1802.

Raasch, S., Franke, T., 2011. Structure and formation of dust-devil-like vortices in the atmospheric boundary layer – a high resolution numerical study. J. Geophys. Res. 116, D16.120.

Raasch, S., Schröter, M., 2001. PALM – a large-eddy simulation model performing on massively parallel computers. Meteorol. Z. 10 (5), 363–372.

Schröter, M., Raasch, S., Bange, J., 2000. Simulated airborne flux measurements in a LES generated convective boundary layer. Bound.-Layer Meteorol. 95, 437–456.

Schumann, U., 1975. Subgrid scale model for finite difference simulations of turbulent flows in plane channels and annuli. J. Comput. Phys. 18, 376–404.

Stull, R.B., 1988. An Introduction to Boundary Layer Meteorology. Kluver Academic Publishers, Dordrecht, p. 666.

Verheij, F.J., Cleijne, J.W., Leene, J.A., 1992. Gust modelling for wind loading. J. Wind Eng. Ind. Aerodyn. 42, 947–958.

Wicker, L.J., Skamarock, W.C., 2002. Time-splitting methods for elastic models using forward time schemes. Mon. Weather Rev. 130, 2088–2097.